Properties of Fullerene-Containing Natural Rubber

B. Jurkowska,[1] B. Jurkowski,[2] P. Kamrowski,[2] S. S. Pesetskii,[3] V. N. Koval,[3] L. S. Pinchuk,[3] Y. A. Olkhov[4]

[1]*Research and Development Center for the Tire Industry (OBR PO), Stomil, 61-361 Poznan, Starolecka 18, Poland*
[2]*Plastic and Rubber Processing Division, Poznan University of Technology, Piotrowo, 3, 60-965 Poznan, Poland*
[3]*V. A.Belyi Metal-Polymer Research Institute (MPRI), National Academy of Sciences, Gomel 246652, Republic of Belarus*
[4]*Institute of the Problems of Chemical Physics, Russian Academy of Sciences, 142 432 Chernogolovka, Moscow Region, Russia*

Received 5 May 2005; accepted 16 July 2005
DOI 10.1002/app.22721
Published online in Wiley InterScience (www.interscience.wiley.com).

ABSTRACT: Addition of fullerene in concentration between 0.065 and 0.75 phr increases Schob elasticity, hardness, and modulus of NR-based rubber. There is no substantial influence of fullerene on T_g, tan δ, and *G*-modulus all evaluated by DMA at twisting within a temperature range −150 to −50°C (glassy state). At temperatures between 0 and 150°C (rubbery state) it is different, namely an increase in modulus and some changes in the slope of segments in *G*(*T*) curves were observed. It could be resulted from additional strong physical junctions of the rubber network. This suggests the growth of degradation energies of the branching junctions and related rise in the aging resistance as concentration of fullerene increases. Simultaneously, it could be expected some reduction of tire temperature at service. Because of this, introduction of fullerene could be reasonable for tread rubbers in case of reduction of its price. Permittivity and dielectric loss angle are correlated with fullerene concentration. Compounding technology when fullerene dispersed within carbon black is mixed with raw rubber on available machines could be easily implemented in the industry. © 2006 Wiley Periodicals, Inc. J Appl Polym Sci 100: 390–398, 2006

Key words: nanocomposite; rubber; NR; fullerene; filler; mechanical properties; electrical properties

INTRODUCTION

Fullerene consists of molecular balls made of 60 (termed C60) or more carbon atom clusters linked together.[1,2] Each of the carbon atoms has two single bonds and one double bond that attach to other carbon atoms. This causes C60 to act more like a "superalkene" than a "superaromatic."[3] The new methods of production of fullerene allow to reduce its cost to $100/kg.[1]

The antioxidant and reactive properties of fullerene make it suitable for use in rubbers especially those exposed to UV lights as they become stronger and more elastic. Aging does not decrease mechanical properties of rubber. Besides, the resistance to high temperature degradation could be improved.[4–7] It is expected that filling with small amount of fullerene could lead to a new set of properties, which has specific advantages over those of rubbers in use. In the present work, rubber containing various concentration of fullerene was tested both at static and dynamic conditions.

EXPERIMENTAL

Materials

Natural rubber (grade SMR 20, Malaysia) containing 0.065–0.75 phr of fullerene was used (Table I). The other additives of rubber compounds have the same concentration in phr against NR content. The ingredients were supplied: ZnO by Metallurgic Plant, Bedzin, Poland; stearic acid by Nitrogen Plant, Kedzierzyn, Poland; Dusantox IPPD by Duslo-Sala, Slovakia; Matoflex TMQ, Hungary; Vulkasil CBS by Duslo-Sala, Slovakia; Duslin PP by Duslo-Sala, Slovakia; and mineral sulfur by Siarkopol, Tarnobrzeg, Poland. All were standard commercial-grade materials.

Preparation of rubber compounds and their vulcanization

A gum compound, taken as a reference, and five compounds with fullerene-containing carbon black have been made in a laboratory Banbury-type internal

Correspondence to: B. Jurkowski (Boleslaw.Jurkowski@put.poznan.pl).
Contract grant sponsor: Polish State Committee of Scientific Research; contract grant number: 4 TO8E 067 25.
Contract grant sponsor: Poznan University of Technology; contract grant number: TB-29-019/2004.

TABLE I
Rubber Compound Formulation

Component	Concentration (phr)
Mixing stage 1	
Natural Rubber (SMR 20)	100
ZnO	5.0
Stearic acid	2.0
Fullerene-containing carbon black[a]	5.0
Dusantox IPPD	1.2
Matoflex TMQ	1.5
Mixing stage 2	
Vulkasil CBS	0.6
Duslin PP	0.2
Mineral sulfur	2.6

[a] Various concentration of fullerene.

mixer (2-L volume, Meccaniche Moderne, Italy) at 40 rpm. The temperature of its chamber at start of mixing was 150°C. The compounding procedure was as follows: loading a raw rubber into the internal mixer, additives: ZnO, stearic acid, Santoflex IP, Flectol H and next, carbon black containing uniformly dispersed fullerene. The batch was dumped at 195°C and then mixed ~15 min with carbon black. At the finishing stage of mixing that lasted 7 min, the curatives were added on the open mill (laboratory-type with a friction ratio of 1:1.14) at a temperature not exceeding 80°C.

The rubber compounds were cured in respective molds in the electrically heated press with a table of 400 mm × 400 mm at 150°C for optimum cure time (t_{90}), which was determined using an oscillating disk rheometer (Monsanto R100, St. Louis, MO); larger specimens were vulcanized 5 min longer than the optimum cure time.

Test methods

Schob elasticity was measured according to ISO 4662: 1986 using rebound resilience tester, Zwick, Germany, model 5109.01.

Static hysteresis was measured at room temperature (21°C) using an Instron 1115 tensile testing machine (Instron Ltd. Corp., High Wycombe Bucks, UK). Loading was performed in 10 cycles running from 0 to 1.8 kN or 1.2 MPa and back to zero at a compression rate of 5 mm/min. Hysteresis loss was measured by subtracting the area under the force-retraction curve from the area under the force-deformation curve. Static hysteresis was calculated as the ratio of hysteresis loss to the area under the force-deformation curve.

Temperature rise and a permanent set (deformation after 25 min of testing, resting time 30 min) were evaluated by using a Goodrich-type flexometer (model FR-2, Metallist, Leningrad, Russia) in which the specimen was compressed at a frequency of 30 Hz at 40°C.

Hardness (Shore A) was measured using tester KA-BID—-PRESS KP 15004, Poland.

Tensile strength, elastic modulus, and elongation at break were measured according to ISO 37:1994 and tear resistance according to ISO 34-1:1994 (an unnotched 90° angle specimen). The Instron 4466 Universal Testing Machine was used to measure these properties.

Aging of the specimens was performed in an air-circulation heating oven operated at 70°C for 168 h, according to ISO 188:1998 (model UT6060, Heraeus Instruments GmbH, Hanau, Germany).

The wetting angle of the specimens by distilled water and medical vaseline oil (VO) has been measured by a special device developed at MPRI. The specimen degreased by alcohol was placed on the movable table, and a drop of a standard liquid was put on its surface from a syringe. After 1 min, the wetting angle was computer-recorded from the image of the drop obtained by a long-focus microscope.

For triboengineering testing, a tribometer with a steel spherical indenter 3 mm in diameter that reciprocated over a 5-mm-long friction path was used. The friction coefficient μ was measured under 0.2 and 0.5 N loads on the indents.

Electro-physical properties, such as permittivity (ε) and the tangent of dielectric loss angle (tan δ), of the specimens were measured according to the Russian State Standard 6433.4-71 using industrial frequency currents (50 Hz). The spectra of thermally stimulated currents (TSC) of the specimens were recorded by a device for thermostimulated depolarization of dielectrics. To characterize ε, tan δ, conductivity G_E, surface resistance R_E , the AC–DC LCR circuit was used. The results are averaged over 5–7 replicate measurements.

The coefficients of reflection R and attenuation S of the electromagnetic radiation passing through the specimens under study were estimated. The scatterometric method and a panoramic indicator (model P2-61) were used to measure the standing-wave factor by the voltage (SWFv). The specimens were placed into a wave-guide path of the indicator and tested under a normal incidence of the electromagnetic wave (EMW) within 8–12 GHz frequency range ν (wavelengths λ = 3.75–2.5 cm). To estimate the reflection coefficient, the specimens were brought into contact with a metal substrate reflecting the radiation and placed into the wave-guide path of the indicator where the SWFv was measured at different ν. The reflection coefficients were calculated by the formula $R = (\text{SWFv} - 1) \times 100/(\text{SWFv} + 1)$, %.

The inverse torsion pendulum (DMA) device designed at MPRI[8-10] was used to determine the dynamic G-moduli, loss moduli, and related tan δ. The specimens in the form of strips (50 × 5 × 0.5 mm^3 in size)

were heated over the temperature range from −150 up to 200°C at a rate of 1.5°C/min. The temperatures were measured within ±0.1°C accuracy. The pendulum twist angle was 3°, and the oscillation frequency was 1 ± 0.01 Hz. Deviations in G measurements were 3–5%.

For thermomechanical analysis (TMA), a UIP-70M apparatus made by the Central Design Bureau of the Russian Academy of Sciences (Moscow) was used. The procedure is as follows: the specimen was put into the measurement cell of the thermostatic chamber. It was frozen without pressing under a scanning rate of about 4°/min, starting from room temperature, usually to −120°C. Next, the specimen was stored for 10–15 min to equalize a thermal field within it. To obtain a thermomechanical curve (TMC), the probe with a stable, but small load is moved down to contact the surface of the specimen and heating is provided.

The TMA allows[11,12] to determine temperatures of the glass transition T_g and the beginning of flow T_f. It is possible to identify several regions in the surface layer of polymers characterized by three states each and differing in linear thermal expansion coefficients in glassy and rubbery states as well as in the zone of melting of the crystalline portion. It also makes possible to evaluate the molecular-weight characteristic of the chain segments between junctions in individual regions. Simultaneously, evaluation of the compaction factor $V_c^{TMA} \approx 3(\alpha_2 - \alpha_1)T_g$ could be done,[12,13] where α_1 is the coefficient of linear thermal expansion in a glassy state = $(\Delta H/H_0)/\Delta T$, where $\Delta H/H_0$ is a relative change in the initial height H_0 (specimen thickness) within the temperature interval, ΔT, α_2 –as α_1, but in rubbery state, T_g is the glass transition temperature. The V_c^{TMA} is related to polymer compactness at nano-, micro-, and macroscale, as well as the free volume fraction. However, little is known about the usability of these characteristics to optimize the composite formulation and processing parameters. It is due to several factors: TMA tests concern surface layers up to 0.5 mm thick,[14] whereas in mechanical measurements, a specimen is usually much thicker depending on the test. This fact influences the gradient of crosslink density of the specimen and both the gradient of crystallinity degree and crystals' sizes distribution if the material is crystallizable. Second are the testing conditions, and third is the material state when testing (solid or dissolved). In spite of all this, only several mechanical characteristics correlate with those from the TMA.[15]

RESULTS AND DISCUSSION

Mechanical properties

The rubbers were soft and very elastic. Addition of fullerene increases Schob elasticity, hardness, and modulus at different elongations (Table II). This situation was expected by analogy with a case when carbon black causes an increase in the effective crosslink density of the rubber network. Accelerated aging increases rubber modulus, but the rate of modulus change is lower for higher fullerene contents.

The permanent set and temperature rise at Goodrich test (Table II), and static hysteresis slightly grow or are independent of the fullerene amount. Static hysteresis, temperature rise, and permanent set at Goodrich test for gum rubbers are much higher, while hardness lowers in comparison with those for the fullerene-containing rubbers. This evidences that physical branching junctions in the rubber network created by fullerene are stronger and are not easy by degradable at testing conditions.

The rate of changes in modulus resulted from accelerated aging expressed by M_{agi}/M (Table II) especially at 0.75 phr fullerene suggests that this filler substantially reduces effects of rubber degradation.

Surface investigations

Wetting of a rubber surface influences the friction-related phenomena at service conditions. To study such phenomenon, the wetting angle Θ of the cured rubber by distilled water and medical VO has been measured (Table III). While water was used, a small amount of fullerene introduced makes the system more hydrophobic. The same conclusion could be made while VO is used. Because of this, it could be supposed that introduction of small amount of fullerene influences tribological properties of the system under investigation.

The wetting angle is virtually independent of concentration of fullerene in the studied interval of concentrations or passes a maximum that corresponds to 0.5 phr (however, being close to the confidence interval of this angle measurements). The equilibrium wetting angle is $\cos\Theta=(\sigma_{sg}-\sigma_{sl})/\sigma_{lg}$, where σ_{sg}, σ_{sl}, and σ_{lg} are surface tension at the solid–gas, solid–liquid, and liquid–gas interfaces, respectively; σ_{lg} = const. Therefore, we may assume that σ_{sg} = const at low filling degree of rubber with fullerene. Consequently, only σ_{sl} is in extreme dependency on the content of fullerene. The reason may be in adsorption of liquid molecules on the specimen surfaces starting from some threshold value. This adsorption results in lowered surface tension σ_{sl}.

In triboengineering test, (Fig. 1) curves $\mu(\tau)$ determined at load P = 0.5 N virtually coincide for all the specimens. At P = 0.2 N, the curve is arranged similarly, but with the maximal concentration of fullerene applied (0.75 phr), the friction coefficient is slightly higher.

TABLE II
Mechanical and Electrical Properties of Cured Rubbers

Properties		Fullerene concentration (phr)					Correlation coefficient, r
		0.065	0.2	0.375	0.5	0.75	
Schob elasticity (%)		65.0 ± 1.4	66.5 ± 0.6	69.0 ± 0.8	72.5 ± 0.9	71.1 ± 0.8	0.88
Permanent set (%)		1.9 ± 0.5	0.9 ± 0.5	0.9 ± 0.2	1.1 ± 0.3	1.1 ± 0.3	−0.5
Temperature rise (°C)		4.3 ± 0.6	5.68 ± 0.8	5.1 ± 1.6	4.3 ± 0.5	4.6 ± 1.0	0
Static hysteresis (%)		10.75 ± 0.6	10.5 ± 0.7	11.6 ± 0.3	10.1 ± 0.5	11.9 ± 0.2	0.5
	Hardness (°Shore A)	28.8 ± 2.5	31.8 ± 2.5	32.7 ± 1.3	33.3 ± 1.6	34.7 ± 1.3	0.94
	Tear resistance (N/mm)	23.8 ± 1.5	27.0 ± 1.2	26.7 ± 1.2	28.5 ± 3.3	29.7 ± 1.7	0.93
Before aging	Modulus at 100% (MPa)	0.59 ± 0.2	0.72 ± 0.2	0.89 ± 0.1	0.96 ± 0.1	1.64 ± 0.4	0.95
	Modulus at 200% (MPa)	1.04 ± 0.2	1.43 ± 0.2	1.52 ± 0.1	1.68 ± 0.1	2.43 ± 0.4	0.97
	Modulus at 300% (MPa)	1.63 ± 0.2	2.43 ± 0.2	2.38 ± 0.1	2.70 ± 0.1	3.48 ± 0.4	0.95
	Hardness (°Shore A)	37 ± 1	39.5 ± 1	39.5 ± 1	40 ± 1	42 ± 1	0.94
	Modulus at 100% (MPa)	0.82 ± 0.1	1.07 ± 0.2	1.06 ± 0.1	1.08 ± 0.1	1.04 ± 0.1	0.59
	$M_{agi}100/M100$	1.39	1.49	1.19	1.13	0.63	−0.94
After aging	Modulus at 200% (MPa)	1.45 ± 0.1	1.94 ± 0.4	1.93 ± 0.2	2.00 ± 0.2	2.01 ± 0.1	0.75
	$M_{agi}200/M200$	1.39	1.36	1.27	1.19	0.83	−0.95
	Modulus at 300% (MPa)	2.35 ± 0.1	3.22 ± 0.6	3.21 ± 0.3	3.33 ± 0.3	3.45 ± 0.2	0.80
	$M_{agi}300/M300$	1.44	1.33	1.35	1.23	0.99	−0.94
Wetting angle Θ, degrees	By water[a]	87	92	92	95	89	0
	By oil[b]	21	20	23	20	10	−0.75
Permitivity ε		4.8 ± 0.1	4.8 ± 0.1	4.9 ± 0.1	5.0 ± 0.1	5.2 ± 0.1	0.97
Dielectric loss angle		0.0035 ± 0.0002	0.0037 ± 0.0002	0.0039 ± 0.0002	0.0043 ± 0.0002	0.0051 ± 0.0002	0.98
Conductivity G_g		$<10^{-10}$	$<10^{-10}$	$<10^{-10}$	$<10^{-10}$	$<10^{-10}$	0
Surface resistance R_g (Ω)		$8.1 \cdot 10^6$	$4.2 \cdot 10^6$	$3.5 \cdot 10^6$	$4.4 \cdot 10^6$	$5.8 \cdot 10^6$	0
Inverse pendulum tester[c]	T_R (°C)	−54.3 ± 0.1	−53.8 ± 0.1	−53.6 ± 0.1	−54.0 ± 0.1	−53.5 ± 0.1	0.71
	$G_{0°C}$ (MPa)	0.50 ± 0.01	0.49 ± 0.01	0.56 ± 0.01	0.56 ± 0.01	0.56 ± 0.01	0.82
	$G_{50°C}$ (MPa)	0.43 ± 0.01	0.51 ± 0.01	0.56 ± 0.01	0.57 ± 0.01	0.60 ± 0.01	0.95
	$G_{100°C}$ (MPa)	0.44 ± 0.01	0.53 ± 0.01	0.56 ± 0.01	0.60 ± 0.01	0.62 ± 0.01	0.93
	$G_{140°C}$ (MPa)	0.49 ± 0.01	0.61 ± 0.01	0.61 ± 0.01	0.67 ± 0.01	0.68 ± 0.01	0.88
	T_{wt} (°C)	225	–	≈220	215	210	–

[a] Measurements error, ± 4.8%.
[b] Measurements error, ±11%.
[c] G is modulus at twisting. [T_g], glass transition temperature; T_{wt}, temperature of the beginning of creation of the second polymer network; M_{agi}/M, ratio of modulus after aging to that initial one for respective elongations.

TABLE III
Characteristics of Molecular and Topological Structures of Rubbers

Analyzed Parameter[a] (95% Confidence Limit)	Fullerene Concentration (phr)					Correlation Coefficient, r
	0.065	0.20	0.375	0.50	0.75	
Low-temperature amorphous region						
T_g, °C (±3–5)	−62	−64	−71	−74	−69	−0.70
$\alpha_1 \times 10^5$ deg^{-1} (±10%)	5.68	6.25	7.35	6.70	6.90	0.70
$\alpha_2 \times 10^5$ deg^{-1} (±10%)	29.9	26.0	23.3	24.7	26.0	−0.52
α_2/α_1	5.26	4.16	3.17	3.69	3.77	−0.65
V_c^{TMA} (±10%)	0.152	0.123	0.097	0.107	0.117	−0.60
$\bar{M}'_{n(n)} \times 10^{-3}$ g/mol (±10%)	53.2	41.4	35.0	19.5	14.1	−0.97
$\bar{M}'_{n(\omega)} \times 10^{-3}$ g/mol (±10%)	85.2	64.2	62.4	37.1	22.8	−0.97
K' (±10%)	1.60	1.55	1.78	1.91	1.61	0
T_∞',°C (±3–5)	64	62	62	74	72	0.74
φ' (±10%)	0.29	0.39	0.34	0.44	0.50	0.90
High-temperature amorphous region						
T_{htt}, °C (±3–5)	120	117	115	109	105	−0.90
$\alpha_3 \times 10^5$ deg^{-1} (±10%)	−55.6	−66.7	−41.7	−48.8	−50.0	0.50
$\bar{M}''_{n(n)} \times 10^{-3}$ g/mol (±10%)	139.7	110.2	96.5	49.1	32.7	−0.97
$\bar{M}''_{n(\omega)} \times 10^{-3}$ g/mol (±10%)	196.2	148.3	133.4	68.1	45.3	−0.97
K'' (±10%)	1.40	1.35	1.38	1.39	1.38	0
T''_∞, °C (±3–5)	210	209	209	213	209	0
φ'' (±10%)	0.71	0.61	0.66	0.56	0.50	−0.90
T_g, °C (±3–5)	215	228	223	231	236	0.87
Values averaged between regions						
$\bar{M}_{n(n)} \times 10^{-3}$ g/mol (±10%)	83.7	54.7	54.3	30.3	20.6	−0.95
K (±10%)	1.96	2.11	2.02	1.77	1.99	0

[a] T_g, temperature of glass transition; T_f, temperature of the beginning of molecular flow; T_∞, temperature of the beginning of the plateau of high-elasticity; T_{htt}, temperature of the high-temperature transition; α_1, coefficient of linear thermal expansion in a glassy state; α_2, as α, but in a rubbery state V_c^{TMA} is compaction factor; α_1, coefficient of linear thermal expansion in a high-elastic state intermediate-temperature region; φ, share of amorphous region; K is the polydispersity index; $\bar{M}_{n(n)}$, number-average molecular weight; $\bar{M}_{n(w)}$, weight-average molecular weight.

Electrical investigations

TSC spectra of the filled rubber specimens do not bear any significant information (charge carrier traps are absent). A distinguishing feature is the appearance of current peaks corresponding to charge relaxation of mechanoelectrets formed when test specimen were cut-off. It is quite evident that with fullerene content between 0.065 and 0.75 phr, ε and tan δ of the specimens augment, too. This is clearly attributed to the presence of fullerene, because carbon black content is identical and small in all specimens (5 phr). The growth of ε proves that polarizability of the specimens goes up, i.e., the charges start to redistribute under the action of the external electric field and the increment of electric dipolar moment in the dielectric redistribute, as well. This is associated, most likely, with growing Maxwell–Vagner's contribution at the fullerene–polymer interface. From this, it is concluded that the extreme dependence of Θ results from two competing factors: reduction of σ_{sl}, i.e., diminished surface energy, and it increased polarizability of rubber.

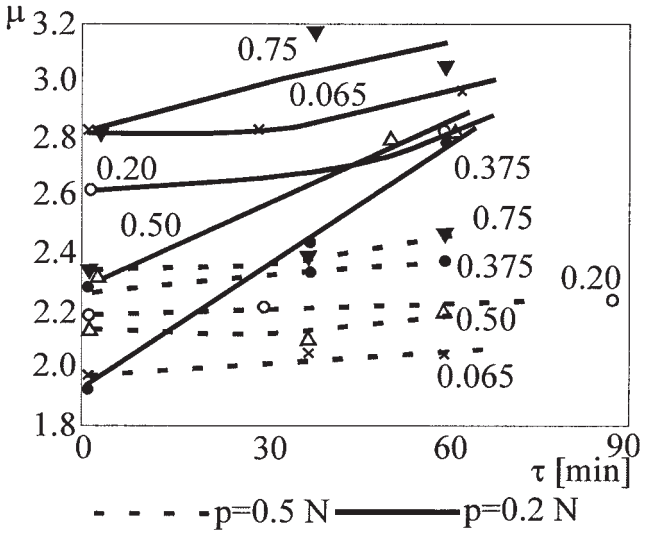

Figure 1 Curves of friction coefficient μ.

The upper curve of radio absorption (Fig. 2) virtually coincides with that of the initial rubber. The specimen with 0.065 phr of fullerene does not influence EMW absorption in any way. On increasing the fullerene concentration, the absorption kinetic changes and the curve $S(\nu)$ transforms to a mirror reflection. The increased fullerene content does not affect S within the studied concentration range, 0.2–0.75 phr. Evidently, its threshold concentration in rubber at which the radio absorp-

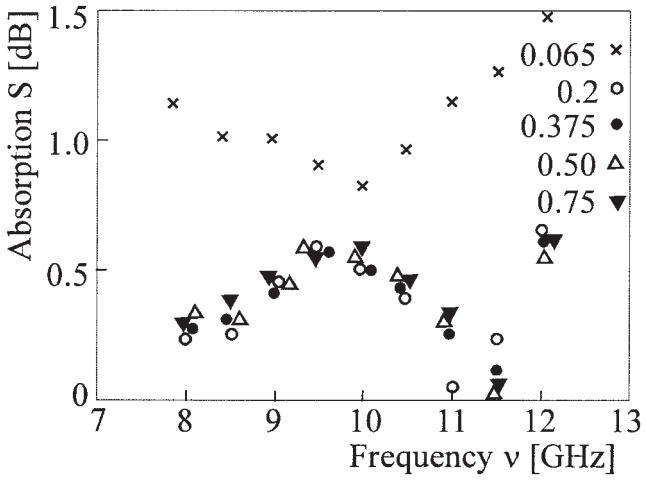

Figure 2 Radio absorption.

tion behavior changes abruptly is somewhere between 0.065 and 0.2 phr.

Structural investigations

At temperatures between −150 and −50°C (glassy state of rubber) when rubber is rigid, *G*-modulus is virtually independent on the fullerene concentrations between 0.065 and 0.75 phr (Fig. 3), and a single major peak of the tan δ plot (Fig. 4) at −54°C typical of T_g^{NR} evidences that fullerene in concentrations studied does not influence the glass transition.

The properties evaluated at temperatures between −50 and 250°C (high-elastic state of rubber) shown in Figures 5 and 6 are different from those discussed previously; now, we could discriminate some regions evidencing that variations in relaxation behavior depend on the concentration of fullerene. For rubbers in a high-elastic state, an increase in fullerene concentration is followed by a rise in modulus (Fig. 5). It is especially visible at temperatures between −10 and

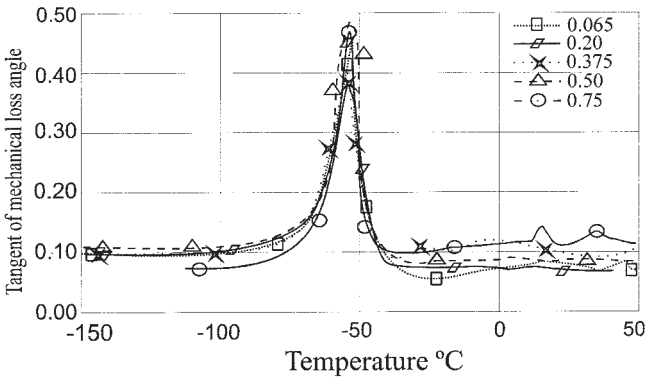

Figure 4 The dependency of tan δ from DMA test at twisting on fullerene concentration for low-temperature range.

150°C (Table II, see $r = 0.82–0.95$). Most likely, it is caused by creation of additional strong physical junctions of the rubber network. Some changes in the slope of segments of *G*(*T*) curves between 0 and 150°C and lowered temperature of the beginning of creation of a second polymer network (recombination of primary crosslinks into structures more stable thermally and chemically) suggest the growth of degradation energies of the branching junctions as concentration of fullerene increases.

The decrease of loss tangent at temperature range between 20 and 150°C in Figure 6 is the lowest for the highest concentration of fullerene. It evidences that part of the branching junctions in the rubber network related to presence of fullerene has high degradation energy as it was supposed earlier.

High tan δ at a low temperature gives a high wet grip, and low tan δ at a moderate temperature (50–70°C) reduces the rolling resistance of tires.[16] This fact and Figure 6 considered together suggest that fullerene introduced even in a small quantity in tread rubber influences positively the traction properties of tires.

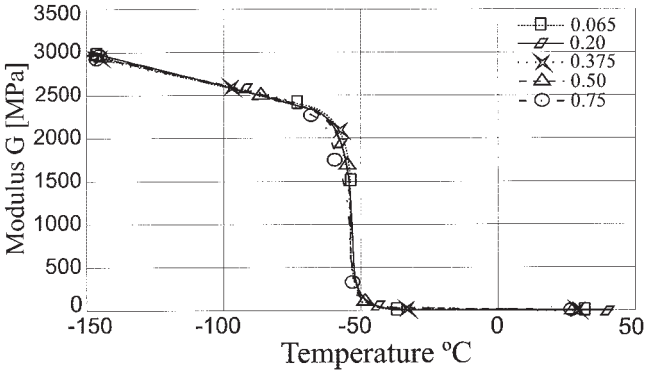

Figure 3 The dependency of modulus from DMA test at twisting on fullerene concentration for low-temperature range.

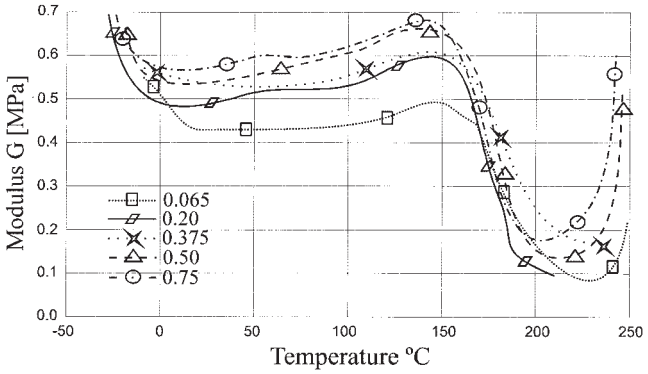

Figure 5 The dependency of modulus from DMA test at twisting on fullerene concentration for high-temperature range.

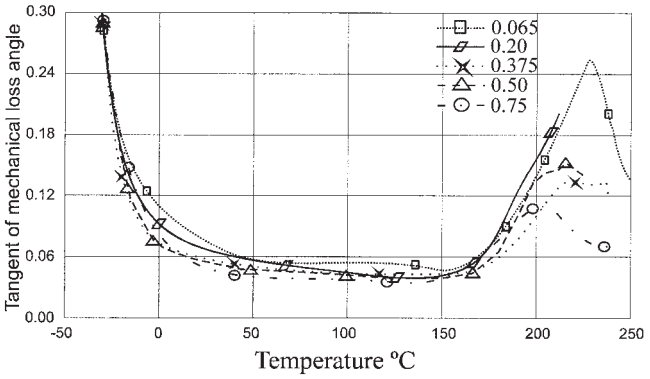

Figure 6 The dependency of tan δ from DMA test at twisting on fullerene concentration for high-temperature range.

The *G*-modulus in temperature range between 140 and 220°C decreases because of some degradation of polymer network, most likely its both strong physical junctions and weak crosslinks. At temperatures above 200°C, there was observed a successive increase in modulus (the highest for a high concentration of fullerene) and tangent of mechanical loss (the lowest for the highest concentration of fullerene). This is an evidence of secondary branching of rubber.

The rubber under investigation has a topological structure with two regions differing in transition temperatures and thermal expansion coefficients; the filler investigated did not influence the number of topological regions, but considerably changed several molecular characteristics of the cured rubber (Table III). This structure maintains till high-temperature transition T_{htt} between 105 and 120°C when there begins the thermal degradation of the physical branching junctions of the network of the high-temperature region. These junctions are presumably formed by associative processes between neighboring segments in natural rubber with trans-configuration and by interactions of the chain segments with active filler. This degradation process terminates at temperature T_{∞}'' when there begins the rubbery state of the high-temperature region. Its value is independent of fullerene concentration while the value for the low-temperature region depends on it.

The shares of topological regions change in a way dependent on rubber formulation.[13,14,17,18] In the case studied, the share of low-temperature region grows and, consequently, the share of high-temperature region lowers as the concentration of fullerene increases ($r = 0.9$).

The ratio of coefficients of linear thermal expansion in a glassy state (α_1) and α_2 –as α_1 but in rubbery state, is virtually independent or slightly dependent on fullerene concentration ($r = -0.65$).

If $6 > \alpha_2/\alpha_1 \geq 2.5$, it implies first of all that the network has branching junctions of a chemical nature. For $\alpha_2/\alpha_1 < 2.5$, the network has junctions of a complex (chemical, physical, and topological) nature.[19] Values of α_2/α_1 in Table III suggest a chemical nature of the branching junctions. However, it is possible to assume that in rubbers under investigation, strong physical interactions occur that are comparable, in degradation energy, with chemical bonds. This structure is not steady[20] and depends on numerous factors, which have not been fully investigated yet.

A pseudonetworked low-temperature amorphous region or soft amorphous fraction (SAF) consists mainly of mobile rubber chain segments. There can also be present a high-temperature amorphous region or rigid amorphous fraction (RAF) consisting of chain segments, which strongly interact with the surface of active filler (carbon black and fullerene), as it reduces essentially the mobility. In addition, zones of interaction with more polar structures in the polymer creating the cluster-type physical junctions between the chains and crystalline structures could be formed. It is postulated that physical networking junctions in SAF are formed by RAF or by unstable microcrystals of near critical size as well as by the chain segments, which do not strongly interact with the surface of filler because they reduce mobility of the chains. The RAF consists of the cluster-type formations, in which the length of chain segments essentially lowers from 140 till 33 kg/mol having the same coefficient of polydispersity along with fullerene concentration grows from 0.065 till 0.75phr. Simultaneously, the share of this region reduces what could be related with increased rigidity of the rubber network that limits a possibility to form successive associative structures of RAF.

The glass-transition temperature is slightly dependent on fullerene concentration (Table III, correlation coefficient $r = 0.7$). A similar conclusion could be made for the thermal expansion coefficients for rubbers in glassy and rubbery states; α_2/α_1 ratio is between 2.5 and 5.12 and it is characteristic of materials in the amorphous state.[11,21,22] The temperature of the beginning of the plateau of high-elasticity of a low-temperature region, T_{∞}', slightly increases as fullerene concentration grows. This suggests some increase in rigidity of the rubber network.

The compaction factor V_c^{TMA}, a value that is inversely proportional to the volume of all voids within the material, for linear soft-chain polymers in the amorphous state $V_c^{TMA} \approx 0.113$, whereas for rigid-chain polymers, which tend to form crystalline structures it is below 0.113.[15,20] For polymer composites $V_c^{TMA} > 0.113$ implying their less compact structure. In the case studied, it has large dispersion (Table III) caused, most likely, by some heterogeneity of rubber and is in the range typical for composites, but a scatter in its values makes impossible to conclude about an influence of fullerene concentration on rubber compactness ($r = -0.6$). An increase in fullerene content is accompanied by a decrease in molecular weight between junctions of a rubber network in both topological regions ($r = -0.97$), which was explained by cre-

TABLE IV
Correlation Coefficients (*r*) Between Structural and Physical Characteristics of Vulcanizate Based on Natural and Fullerene-Containing Carbon Black[a]

Correlated Values	φ'	$\bar{M}'_{n(n)}$	K′	φ''	$\bar{M}''_{n(n)}$	K″	$\varphi'/\bar{M}'_{n(n)}$	$\varphi''/\bar{M}''_{n(n)}$	$\varphi'/\bar{M}'_{n(n)}+\varphi''/\bar{M}''_{n(n)}$	$\bar{M}_{n(n)}=\varphi'\bar{M}'_{n(n)}+\varphi''\bar{M}''_{n(n)}$
M100	0.86	−0.87	0	−0.86	−0.87	0	0.95	0.94	0.95	−0.86
M200	0.92	−0.91	0	−0.92	−0.91	0	0.95	0.94	0.95	−0.91
M300	0.83	−0.85	0	−0.83	−0.82	−0.50	0.68	0.66	0.68	−0.85
M200-M100	0.93	−0.86	0	−0.93	−0.85	−0.52	0.77	0.73	0.76	−0.88
M200/M100	0	0.63	0	0	0.64	−0.51	−0.74	−0.78	−0.76	0.60
Static hysteresis	0	0	0	0	0	0	0	0	0	0
Permanent set	−0.52	0.54	0	−0.52	0	0.71	0	0	0	0.54
Temperature rise	0	0	0	0	0	−0.93	0	0	0	0
Schob elasticity	0.79	−0.95	0.70	−0.79	−0.94	0	0.80	0.84	0.81	−0.94
Permittivity	0.86	−0.92	0	−0.86	−0.93	0	0.98	0.99	0.98	−0.91
Dielectric loss angle	0.91	−0.93	0	−0.91	−0.94	0	0.99	0.98	0.99	−0.93
Tear resistance	0.96	−0.96	0	−0.96	−0.95	0	0.89	0.87	0.88	−0.97
Hardness	0.89	−0.95	0	−0.89	−0.93	0	0.83	0.83	0.88	−0.94

[a] φ' and φ'' are shares of low- and high-temperature regions, $\bar{M}'_{n(n)}$ and $\bar{M}''_{n(n)}$ are number-average molecular weights of chain segments between the junctions in low- and high-temperature regions, respectively, the averaged between regions $\bar{M}_{n(n)} = \varphi'\bar{M}'_{n(n)} + \varphi''\bar{M}''_{n(n)}$, *K* is the polyd ispersity index, $\varphi'/\bar{M}'_{n(n)}$ is crosslink density in low-temperature region and $\varphi''/\bar{M}''_{n(n)}$ that in high-temperature region; in bold are given values ≥0.7.

ation of additional physical junctions. The fullerene particles possibly create high-temperature resistant junctions, which is proved by the growth of temperature of the beginning of flow T_f ($r = 0.87$).

In cured-gum rubber, a spatial structure is arranged mainly due to both the chemical reactions of the curing system and the cluster-type junctions, being degraded at a temperature lower than that for chemical bonds. Introduction of carbon black and fullerene into the rubber could destroy the energetic balance of intermolecular interactions existing there before compounding. However, in filled rubbers, new junctions are created, especially with participation of fullerene. Now, conditions to create the cluster-type junctions having degradation energy on the level as those in a case without active filler are disturbed. As concentration of fullerene increases, stronger rubber/fullerene branching junctions, having higher degradation temperature than that for rubber/carbon black one are expected. They enhance the concentration of junctions in the high-temperature region and its transition temperature determined by TMA, but not at inverse pendulum testing.

Correlation between investigated parameters

In the case studied, changes in the rubber structure are resulted mostly from variation in the share of strong physical junctions caused by fullerene. Stresses at different elongations, usually at 100, 200, and 300% (*M*100, *M*200, and *M*300) are treated in the industry as values related to elastic modulus. Such modulus evaluated at static conditions correlates (Table IV) with the share of low-temperature (φ') and, consequently, also of high-temperature (φ'') regions, because $\varphi'' = 1 - \varphi'$ and, as it was shown in previous investigations,[15] to the number-average molecular weight between the junctions $M_{n(n)}$ in particular topological regions. It correlates also with crosslink density, in particular, topological regions and in the whole specimen; the latter fact is in agreement with well-known results from standard tests.

The (*M*200 − *M*100) value is sometimes used as an indirect measure of elastic modulus being less dependent on preliminary stress during fixing the specimen in the tensile testing machine. Now, a higher correlation coefficient of the (*M*200 − *M*100) value with the share of the regions, the number-average molecular weight of the chain segments included in the regions ($r = -0.85$) and the crosslink density there ($r \approx 0.75$) has been obtained. These correlation coefficients are very close to those determined for particular modules, which suggests that preliminary stress during fixing of the specimen has negligible influence on the conclusions from tensile measurements.

The ratio of *M*200/*M*100 could also be used to describe some changes in elastic modulus resulted from changes in manufacturing technology. However, in the case discussed, this value does not correlate with the share of the regions and polydispersity of the chain segments between junctions in the network of the regions, but it correlates with the effective crosslink density as it was expected based on well-known results from standard tests.

Rubber hardness (Shore A method), tear resistance, and electrical properties correlate with the shares of particular regions ($r \approx 0.9$), the number-average molecular weight between the junctions ($r \approx 0.9$) and crosslink density in these regions ($r \approx 0.9$), and as a result, with molecular weight in entire specimen that is strong ($r > 0.9$). Simultaneously, it is not correlated with the poly-

dispersity index of the chain segments between the junctions of rubber network in both regions.

Schob elasticity being an indirect measure of dynamic losses correlates with all molecular characteristics evaluated, except for the polydispersity index of the high-temperature topological region.

Static hysteresis does not correlate with any molecular characteristics evaluated. This suggests that additional physical junctions formed by fullerene are so strong that they are not degraded at compression testing. The temperature rise in the Goodrich test correlates with the polydispersity index of the high-temperature topological region only. It is independent of the crosslink density and shares of the regions. This fact supports the above-mentioned conclusion about the strength of the junctions formed by fullerene.

The correlation of permanent set in the Goodrich test with the shares of topological regions, the number-average molecular weight between junctions in a low-temperature amorphous region and the crosslink density is absent or is disputable. It is substantial with the polydispersity index of the high-temperature topological region only.

Analyzing the above-mentioned results of calculations, one should keep in mind that because of the limited number of experimental points, some dispersion in the coefficients of correlation against values expected for a larger amount of experimental data should be considered.

CONCLUSIONS

Addition of fullerene increases elastic modulus at different elongations, Schob elasticity, and hardness of cured rubber to a degree that depends on fullerene content. Fullerene significantly reduces the effect of accelerated aging of rubber. Simultaneously, there is no visible influence of fullerene concentrations on T_g, tan δ, and *G*-modulus within a temperature range −150 to −50°C when rubber is rigid.

At temperatures between 0 and 150°C, when rubber is in a high-elastic state, an increase in elastic modulus was explained by creation of additional strong physical junctions of rubber network. Some changes in the slope of segments of curves $G(T)$ and a value of loss tangent independent of amount of fullerene were noticed, but the lowest loss tangent is for the highest concentration of fullerene. This suggests the growth of degradation energies of the branching junctions and related increase in the aging resistance with fullerene concentration. Simultaneously, there could be expected some reduction of tire temperature at service. Because of this, introduction of fullerene could be reasonable for tread rubbers in case of reduction of its price.

The extreme dependence of the equilibrium wetting angle could result from two competing factors: diminishing surface energy and increasing polarizability of rubber. Introduction of small amounts of fullerene influences tribological properties of the system under investigation. At load 0.2 N for the maximal concentration of fullerene applied (0.75 phr) the friction coefficient is slightly higher. Permittivity and dielectric loss angles correlate with the fullerene concentrations.

These conclusions are based on the experiments where fullerene was introduced in concentration varied between 0.065 and 0.75 phr in natural rubber grade SMR 20. Further change in the properties could also occur at higher concentration of fullerene, but the cost of rubber compound would be much higher. The observed trends in changes of rubber properties are in agreement with the published data.

Compounding technology, where fullerene dispersed within carbon black is mixed with raw rubber on available machines could be easily implemented in rubber industry. However, an increase in the batch temperature up to 195°C during compounding was noticed, and so, it is suggested us to use in further experiments, a more effective cooling system because high temperatures may induce a harmful degradation of polymers.

References

1. Murayama, H.; Tomonoh, S.; Alford, J. M.; Karpuk, M. E. Fullerene, Nanotubes, and Carbon Nanostructures 2004, 12, 1.
2. Kroto, H. W.; Heath, J. R.; O'Brien, S. C.; Curl, R. F.; Smalley, R. E. Nature 1985, 318, 162.
3. Birkett, P. R.; Hitchcock, P. B.; Kroto, H. W.; Taylor, R.; Walton, D. R. M. Nature 1992, 357, 479.
4. Hamed, G. R. Rubber Chem Technol 2000, 73, 524.
5. Rus. Pat. 2,151,781 (2000) Institute of the Problems of Chemical Physics, Russian Academy of Sciences.
6. Cataldo, F.; Fullerene, Nanotubes, and Carbon Nanostructures 2001, 9, 497.
7. Cataldo, F.; Fullerene, Nanotubes, and Carbon Nanostructures 2001, 9, 515.
8. Pesetskii, S. S.; Fedorov, V. D.; Jurkowski, B.; Polosmak, N. D. J Appl Polym Sci 1999, 74, 1054.
9. Pesetskii, S. S.; Jurkowski, B.; Koval, V. N. J Appl Polym Sci 2000, 78, 858.
10. Pesetskii, S. S.; Jurkowski, B.; Storozhuk, I. P.; Koval, V. N. J Appl Polym Sci 1999, 73, 1823.
11. Jurkowski, B.; Jurkowska, B.; Andrzejczak, K. Polym Test 2002, 21, 135.
12. Boyer, R. F. Rubber Chem Technol 1963, 36, 1303.
13. Simha, R.; Boyer, R. F. J Chem Phys 1962, 37, 1003.
14. Zielnica, J.; Wasilewicz, P.; Jurkowski, B.; Jurkowska, B. Thermochim Acta 2004, 414, 255.
15. Jurkowska, B.; Jurkowski, B.; Olkhov, Y. A. J Therm Anal Calorim 2005, 81, 27.
16. Donnet, J. B. Compos Sci Technol 2003, 63, 1085.
17. Lipatov, Y. S. Physical Chemistry of Filled Polymers (in Russian); Khimia: Moscow, 1977; p 111.
18. Kuleznev, V. N.; Igosheva, K. M. Vysokomol Soedin 1962, 4, 1858.
19. Olkhov, Y. A.; Gorbushkina, G. A.; Baturin, S. M. Rus. Pat. 1,713,359 A1 (11 Sept. 1989).
20. Hill, A. J.; Zipper, M. D.; Tant, M. R.; Stack, G. M.; Jordan, T. C.; Schultz, A. R. J Phys: Condens Mater 1996, 8, 3811.
21. Olkhov, Y. A.; Jurkowski, B. J Therm Anal Calorim 2005, 81, 489.
22. Bukhina, M. F. Technical Physics of Elastomers (in Russian); Khimia: Moscow, 1984; p 54.